Modern Physics Letters B
Vol. 27, No. 16 (2013) 1350120 (10 pages)

DOI: 10.1142/S0217984913501200

World Scientific
www.worldscientific.com

GROUND STATE ENERGY LEVELS OF INDIUM ARSENIDE QUANTUM DOTS CALCULATED BY A SINGLE BAND EFFECTIVE MASS MODEL USING REPRESENTATIVE STRAINED INPUT PROPERTIES

HYUNHO SHIN

Department of Materials Engineering, Gangneung-Wonju National University, Jughun-gil 7, Gangneung, Gangwon-do 210-702, Republic of Korea
hshin@gwnu.ac.kr

JONG-BONG KIM*

Department of Mechanical and Automotive Engineering, Seoul National University of Science and Technology, Gongneung-ro 232, Nowon-Gu, Seoul 139-743, Republic of Korea
jbkim@seoultech.ac.kr

Received 3 April 2013
Revised 3 May 2013
Accepted 7 May 2013
Published 6 June 2013

Representative strained values of effective mass and potential of charge carriers in indium arsenide (InAs) quantum dots have been used as input to the complete orthonormal set approach of an effective-mass, single-band, and constant-potential model for the calculation of the ground state energy levels. Even with the avoidance of the diagonalization of the strain Hamiltonian matrix, the single-band-model-calculated ground state energy levels are reasonably refined by the use of representative strained values of potential and effective mass.

Keywords: InAs quantum dot; energy level; single-band model.

PACS Number(s): 71.15.Ap, 73.21.La

1. Introduction

Various sizes, shapes, and chemical compositions of indium arsenide (InAs) quantum dots (QDs) embedded in a wide-band gap gallium arsenide (GaAs) barrier are available.[1–4] Theoretical analysis of their energy levels[5–10] is not a simple task, due to the finite potential barrier (often of the order of a few hundred meV), the nontrivial geometry of the QD, and the strain modification of the effective masses

*Corresponding author.

and potentials of charge carriers, which requires the procedure of solving strain Hamiltonian. Subsequently, the numerical procedure is quite often rendered inaccessible to experimentalists, who have to resort to a sort of interpolation of the few cases of published theoretical data in order to interpret or analyze their spectra from obviously different QDs in several terms including size, shape, aspect ratio, areal density of dots, and vertical stacking period. This limitation necessitates a simple model, but nevertheless accurate in comparison with a more sophisticated ones.

Another aspect necessitating a simple model lies in the fact that the experimentally characterized dimension and shape of the QDs, e.g. pyramid, truncated pyramid, lens, hemisphere, are highly uncertain. Thus, only limited dimensions, i.e. base and height dimensions, are often reported, or the dimension and shape of QDs are even omitted in the literature.[4] For a given volume of quantum dots (e.g. 750 nm^3), the uncertainty of QD shape yields ground state transition energy as different as 150 meV.[11] Under such circumstances, resorting to a computationally demanding procedure to seek the energy levels of QDs with uncertain shape and dimension would not be desirable (only quantum dots with minimal uncertainty would deserve such a demanding calculation). Instead, like the works by Marzin *et al.*[1] and Rudno-Rudziski *et al.*,[12] it is first highly desirable to reversely estimate the shape and dimension of the QDs by comparing the experimentally observed photoluminescence data with the calculated energy levels of QDs obtained by assuming a series shape and dimension parameters. For such purpose, the simple and handy model (but nevertheless accurate in comparison with a more rigorous model) is indispensible.

In this sense, the complete orthonormal set (COS) approach of the single band model, with position-independent potential and effective mass, attracts high interest. This model was originally used to calculate the energy levels of charge carriers in a quantum well by Gershoni *et al.*,[13] applied successfully for cuboidal quantum dots by Gangopadhyay and Nag,[14] and extended to pyramidal quantum dots by Califano and Harrison.[15] This approach can be applied to QDs with arbitrary shapes. Because of the position independency of the parameters, no strain Hamiltonian matrix is diagonalized to solve the Schrödinger equation, and thus the computational burden is greatly reduced. However, the well-known lattice-strain-induced modifications[16–20] of potential and effective mass of charge carriers are neglected.

Nevertheless, the influence of strain could be accounted for if the representative strained values of the effective mass and confining potential are used as input for each of the QDs with different shapes and aspect ratios under different strain conditions. Therefore, it is very interesting to investigate whether or not the use of the representative strained input properties for each QD by the COS approach is capable of predicting comparable energy levels to the ones based on theoretically more sophisticated models. Under the spirit of the current work seeking a handy but accurate model, it is also noted that Zora *et al.*[21] developed a set of luminescence equations by solving Schrödinger equation without including the strain

Hamiltonian. Under quasi-equilibrium conditions, the set of luminescence equations become a closed-set of equations to predict the emission spectra of QDs with arbitrary shapes. The validity of the model was proven for single QD. The use of the strain modified potentials and effective masses as input for their model would also be informative for the application of the model to QDs under various strain conditions.

As for the calculation of the strain-modified energy levels of various quantum dots by the complete orthonormal set (COS) approach of the single band model, to date, efforts have been made only to seek a universal set of strained input values (potentials and effective masses) for various quantum dots by using only quantum dot dimension (height and base) as input parameters.[15] However, it is apparent that the process of seeking strain-modified input properties (potential and effective mass) is indispensable for each comparing QD to calculate energy levels because the strained properties vary significantly depending on variables including the aspect ratio, shape, composition, areal density of QDs, and especially the vertical stacking period: no universal set of strained input properties exists for such versatile QDs. The process of seeking strain for each comparing QD should impose only a mild burden because the simple continuum elasticity approach is valid down to one monolayer thin films.[22,23] Then, the representative strain-modified input properties, e.g. the ones along QD-axis, can be readily obtained from the strain information via simple analytical relations based on the model solid theory[24] or the result of 8-band $k \cdot p$ theory.[25]

Here, we seek a comparison of the calculated result via the COS approach of the single-band, effective-mass, constant-potential model by using representative strained input properties with other calculation results based on theoretically more sophisticated models in the literature, rather than with experiments elsewhere. This approach is adopted because comparisons with experiments may lead to a fortuitous coincidence of energy levels due to the well-known uncertainty in the experimentally determined QDs (shape and dimension).

2. Numerical Analysis

Briefing the complete orthonormal set (COS) approach, the envelope function $\Psi(x, y, z)$ of the Schrödinger equation for the position-dependent effective mass and potential,

$$-\frac{\hbar^2}{2}\left(\nabla\frac{1}{m(x,y,z)}\nabla\right)\Psi(x,y,z) + V(x,y,z)\Psi(x,y,z) = E\Psi(x,y,z) \qquad (1)$$

is expanded by a COS of solutions of the cuboidal problem with infinite barrier height,[13,14] i.e.

$$\Psi(x,y,z) = \sum_{lmn} a_{lmn}\psi_{lmn}(x,y,z)\,, \qquad (2)$$

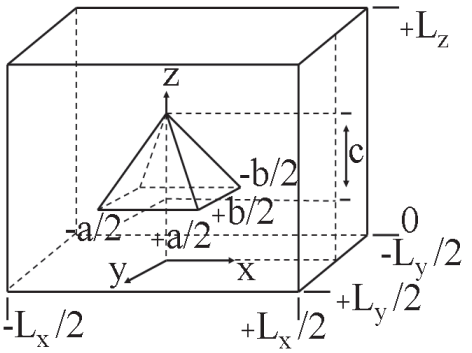

Fig. 1. Geometry for the calculation.

where[15]

$$\psi_{lmn}(x,y,z) = \sqrt{\frac{2}{L_x}}\sin\left[l\pi\left(\frac{1}{2}-\frac{x}{L_x}\right)\right]\sqrt{\frac{2}{L_y}}\sin\left[m\pi\left(\frac{1}{2}-\frac{y}{L_y}\right)\right]$$
$$\times\sqrt{\frac{2}{L_z}}\sin\left(n\pi\frac{z}{L_z}\right). \tag{3}$$

In Eq. (3), L is the system boundary of the cuboid in each direction (x, y and z denoted as subscripts) as seen in Fig. 1, and subscripts l, m and n are quantum numbers in each direction. Although the COS approach can be applied to QDs with arbitrary shapes, pyramidal QD (Fig. 1) has been selected for comparison of the current result with existing calculations.[5–10] Energy levels of charge carriers in quantum dots are calculated by solving the eigenvalue equation,[13–15]

$$\left(A_{lmnl'm'n'} - E\delta_{l'l}\delta_{mm'}\delta_{nn'}\right)a_{lmn} = 0 \tag{4}$$

and $A_{lmnl'm'n'}$ matrix can be described by

$$A_{lmnl'm'n'} = \left[\frac{\hbar^2\pi^2}{2m_{\mathrm{BR}}}\left(\frac{l'l}{L_x^2}+\frac{mm'}{L_y^2}+\frac{nn'}{L_z^2}\right)+V_{\mathrm{BR}}\right]\delta_{l'l}\delta_{mm'}\delta_{nn'}$$
$$+\frac{\hbar^2}{2}\left(\frac{1}{m_{\mathrm{QD}}}-\frac{1}{m_{\mathrm{BR}}}\right)\times\int_{\mathrm{QD}}\nabla\psi^*_{l'm'n'}\nabla\psi_{lmn}dV$$
$$-V\times\int_{\mathrm{QD}}\psi^*_{l'm'n'}\psi_{lmn}dV \tag{5}$$

using the position-independent effective mass of the charge carriers (electrons and holes), m, and the position-independent potential height of the barrier with respect to the quantum dot region, V. The subscripts BR and QD stand for gallium arsenide (GaAs) barrier and indium arsenide (InAs) quantum dot, respectively.

The values of the integrals in the $A_{lmnl'm'n'}$ have been simply obtained by the Simpson's 1/3 numerical approximation.[26] Care has been taken to move boundaries

Table 1. Strained material parameters used for calculation.

	V (meV)	m_{InAs}	m_{GaAs}
Electron	448	$0.055\mathrm{m}_o$	$0.0665\mathrm{m}_o$
Hole	232	$0.59\mathrm{m}_o$	$0.09\mathrm{m}_o$

L_x, L_y and L_z away from the pyramid, so that the energy eigenvalues are essentially independent of their choice. In the process of expanding the envelope function, a basis of 19 wave functions in each direction was enough to achieve the convergence. Then, the eigenvalue equation was solved, where $A_{lmnl'm'n'}$ is a 6859×6859 matrix, by using standard mathematical software such as MATLAB. The input material parameters used to calculate the energy levels of the charge carriers in pyramidal quantum dots are listed in Table 1. The input values in Table 1 are explained in next section.

3. Results and Discussion

In order to determine the representative effective masses and confinement potentials of charge carriers, strain profiles along quantum dot axis were first calculated by continuum elasticity approach (finite element analysis).[17–20] Then, from the obtained strain profiles, electron effective mass and potentials were determined by the analytical relations based on model solid theory[24] and the results are shown in Figs. 2 and 3, for the case when the quantum dot height is 6 nm and the base is 12 nm. Provided the quantum dot aspect ratio [= height/(base/2)] was the same, no appreciable difference existed in light of the potentials and electron effective mass for QDs with different volumes. For comparison with existing theoretical works,

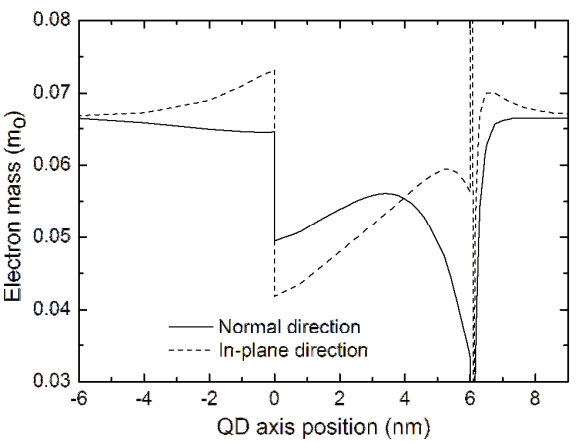

Fig. 2. Change in electron mass along quantum dot (QD) axis position (position zero is the base of the quantum dot).

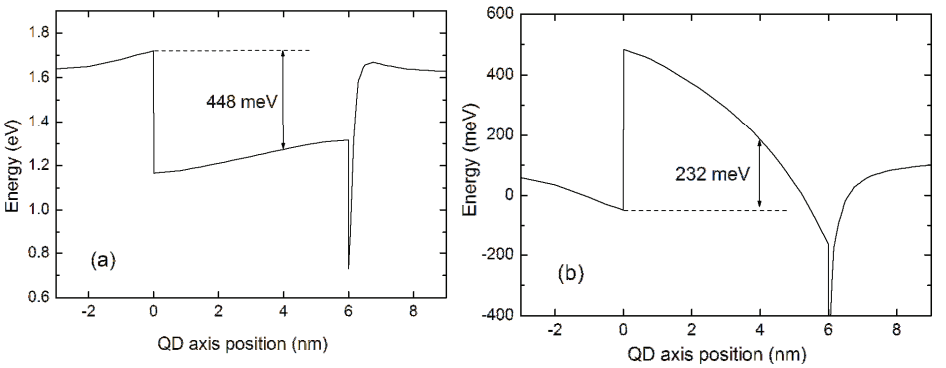

Fig. 3. Changes in potential energy of (a) electron and (b) heavy hole along the axis position of the quantum dot (QD). Position zero is the base of the quantum dot and energy scale is with respect to the unstrained gallium arsenide (GaAs) valence band edge.

different volume quantum dots with aspect ratio of unity have been investigated in the current work.

The singularity of strain itself at around the top apex of the pyramidal QD is well documented,[27,28] which disappears for truncated,[17–20] hemisphere-, and lens-shaped QDs. Because the profiles of effective mass and potential are given as analytical functions of strain,[24,25] they also show the singularity at around the top apex of the pyramid, as seen in Figs. 2 and 3. In finite element analysis, the simulation of strain singularity (the peak height) depends on how finely the space is discretized. Thus, the strain singularity-induced peaks in Figs. 2 and 3 have been truncated for the detailed description of the profiles of effective mass and potential within and around the QD.

As seen in Fig. 2, the electron effective masses in QD along in-plane direction ($m_{e,p,\mathrm{InAs}}$) and normal (growth) direction ($m_{e,n,\mathrm{InAs}}$) are different and vary along the QD-axis. In the current model, which aims at simplicity of the model (but not necessarily with less reliability or less accuracy), the direction dependency of the effective mass is unified to a position-independent representative value in the QD. Also, as seen in Fig. 3, the potentials for charge carriers vary along QD-axis. Thus, it is necessary to select a representative and position-independent value. In the process of selecting representative values of effective mass and potential of charge carriers inside the QD, the singularity-induced peak values at the top apex of the pyramid can be neglected because the probability density of the charge carriers is negligible near the apexes of the pyramid.[9] Further, although strain induces piezoelectric potential, this possibility generally affects the energy levels involved in optical transitions less than 1 meV[5]: thus, it can be neglected.

In Fig. 2, the electron effective masses in quantum dot along in-plane direction ($m_{e,p,\mathrm{InAs}}$) and normal (growth) directions ($m_{e,n,\mathrm{InAs}}$) are the same at approximately the 2/3 position of the quantum dot height. In the current work,

the direction-independent representative effective mass (for electron) was taken at the 2/3 position of the quantum dot height and the representative confinement potential for electron in QD was also taken in that position with reference to the quantum dot base: $m_{e,p,\mathrm{InAs}} = m_{e,n,\mathrm{InAs}} = m_{e,\mathrm{InAs}} = 0.055\mathrm{m}_o$ (m_o is the mass of free electron) and $V_e = 448$ meV [see Fig. 3(a)]. It is true that the determined representative and position-independent values in this way is arbitrary, but the selected ones have to ensure reliable energy levels of the charge carriers after comparison with theoretically more sophisticated models. In the current work, we aim to demonstrate that the selection of the representative values in this way yields reasonably accurate results. Selection of the representative strain-modified values at other heights of QD can also be pursued if necessary.

Since the strain-modification of the electron effective mass is not significant in the GaAs region, the unstrained value of $0.0665\mathrm{m}_o$ ($= m_{e,\mathrm{GaAs}}$)[7] was used. As for the properties of holes, the confinement potential of the hole in quantum dot was also taken at the 2/3 position of the height along quantum dot axis as well from Fig. 3(b): $V_h = 232$ meV. As the influence of strain on effective mass of heavy holes in quantum dot is not described by a simple analytical expressions, the effective mass of heavy hole along [100] direction was taken based on existing pseudopotential calculation:[11] $m_{h,n,\mathrm{InAs}} = m_{h,\mathrm{InAs}} = 0.59\mathrm{m}_o$. Finally, $m_{h,\mathrm{GaAs}} = 0.09\mathrm{m}_o$ was used in the current work as a fitting parameter.

After selecting appropriate representative strain-modified constants (effective mass and potential of charge carriers) as above, Eq. (4) was solved by using the selected constants as input, and the calculated ground state energy level of electron in pyramidal quantum dot is shown in Fig. 4(a) as a function of the base dimension of the quantum dot. Included in Fig. 4(a) are the results obtained by other sophisticated calculations in the literature.

The ground state energy levels in the current work are fairly close to the lower bound of the existing calculations. In the base dimension range between 12 nm and 20 nm, the single-band-constant-potential-model herein predicts the results of Barker and O'Reilly[10] fairly accurately, who calculated the ground state energy levels by solving the strain Hamiltonian. The results in the current work in the range between 11 nm and 20 nm are also similar to those of Stier *et al.*,[9] who calculated the energy levels using 8-band $k \cdot p$ theory. In the base dimension range between 6 nm and 12 nm, the current work predicts fairly closely the results of Grundman *et al.*,[5] who also calculated the ground state energy levels by using position-dependent potentials in single-band effective mass approximation. From above, although position-independent and representative strain-modified potentials and effective masses are used, the current work predicts fairly closely the lower bound of other sophisticated calculations for electrons.

The calculated ground state energy level of heavy hole is now shown in Fig. 4(b) as a function of the base dimension of the quantum dot. Included in Fig. 4(b) are the results obtained by other sophisticated calculations in the literature. Note that a

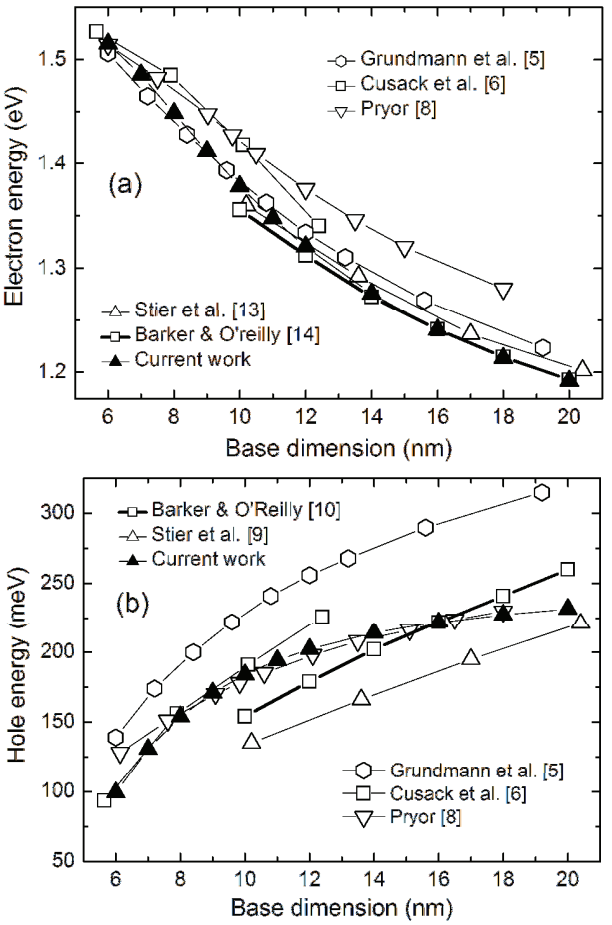

Fig. 4. Ground state energy levels of (a) electrons and (b) heavy holes as a function of base dimension of the pyramidal quantum dots. Energy scale is with respect to the unstrained gallium arsenide (GaAs) valence band edge.

significant percentage of error of heavy-hole energy levels exists among the existing sophisticated calculations themselves, as compared to the electron energy levels [Fig. 4(a)]. In Fig. 4(b), the current work does not predict the lower bound of all of the existing heavy-hole energy levels, unlike the case of the electrons. However, the current work predicts the lower bound of the two existing sophisticated calculations by Pryor[8] and Cusack *et al.*[6] In the base dimension range between 8 nm and 18 nm, the current work predicts fairly closely the lower bound results of Pryor[8] who calculated hole energy levels using 8-band $k \cdot p$ theory. In the range of the relatively small base dimension between 6 nm and 10 nm, the current work is consistent with the lower bound results of Cusack *et al.*,[6] who calculated hole energy levels using a multi-band effective mass theory.

4. Conclusion

When appropriate strained values of effective masses and potentials are used as input, the complete orthonormal set approach of the single-band, effective-mass, constant-potential model predicts fairly reliable energy levels of indium arsenide (InAs) quantum dots embedded in gallium arsenide (GaAs) barrier as compared to other more sophisticated theoretical calculations in the literature. Even with the avoidance of the diagonalization of the strain Hamiltonian matrix, the use of strained representative values of potentials and effective masses as input to the model is a reasonable approach to achieve the ground state energy levels of the charge carriers.

Acknowledgments

This work was supported financially by the Basic Science Research Program (2010-0004150), funded by the Ministry of Education, Science and Technology through the National Research Foundation of Korea (NRFK).

References

1. J. P. McCaffrey, M. D. Robertson, S. Fafard, Z. R. Wasilewski, E. M. Griswold and L. Madsen, *J. Appl. Phys.* **88** (2000) 2272.
2. J. H. Lee, Z. M. Wang, B. L. Liang, K. A. Sablon, N. W. Strom and G. J. Salamo, *J. Phys. D: Appl. Phys.* **40** (2007) 198.
3. J. T. Nag, U. Bangert and M. Missous, *Semicond. Sci. Technol.* **22** (2007) 80.
4. K. H. Schmidt, G. Medeiros-Ribeiro, M. Oestreich, P. M. Petroff and G. H. Döhler, *Phys. Rev. B* **54** (1996) 11346.
5. M. Grundmann, O. Stier and D. Bimberg, *Phys. Rev. B* **52** (1995) 11969.
6. M. A. Cusack, P. R. Briddon and M. Jaros, *Phys. Rev. B* **54** (1996) R2300.
7. M. A. Cusack, P. R. Briddon and M. Jaros, *Phys. Rev. B* **56** (1997) 4047.
8. C. Pryor, *Phys. Rev. B* **57** (1998) 7190.
9. O. Stier, M. Grundmann and D. Bimberg, *Phys. Rev. B* **59** (1999) 5688.
10. J. A. Barker and E. P. O'Reilly, *Phys. Rev. B* **61** (2000) 13840.
11. Y. Li, O. Voskoboynikov, C. P. Lee, S. M. Sze and O. Tretyak, *J. Appl. Phys.* **90** (2001) 6416.
12. W. Rudno-Rudzinski, K. Ryczko, G. Sek, J. Misiewicz, M. J. da Silva and A. A. Quivy, *Solid State Commun.* **135** (2005) 232.
13. D. Gershoni, H. Temkin, G. J. Dolan, J. Dunsmuir, S. N. G. Chu and M. B. Panish, *Appl. Phys. Lett.* **53** (1988) 99.
14. S. Gangopadhyay and B. R. Nag, *Nanotechnology* **8** (1997) 14.
15. M. Califano and P. Harrison, *Phys. Rev. B* **61** (2000) 10959.
16. E. H. Li, *Physica E* **5** (2000) 215.
17. H. Shin, W. Lee and Y.-H. Lee, *Nanotechnology* **14** (2003) 742.
18. H. Shin, K. S. Hong, W. Lee and Y.-H. Yoo, *Surf. Sci.* **652** (2004) 73.
19. H. Shin, K. S. Hong, W. Lee and Y.-H. Yoo, *Appl. Phys. A* **81** (2005) 715.
20. Y. Liu, Z. Yu and Y. Huang, *Int. J. Mod. Phys. B* **20** (2006) 4899.
21. A. Zora, C. Simserides and G. P. Triberis, *J. Phys.: Condens. Matter* **19** (2007) 406201.
22. J. E. Bernard and A. Zunger, *Appl. Phys. Lett.* **65** (1994) 165.

23. D. A. Faux, G. Jones and E. P. O'Reilley, *Model. Simul. Mater. Sci. Eng.* **2** (1994) 9.
24. C. G. Van de Walle and R. M. Martin, *Phys. Rev. B* **34** (1986) 5621.
25. M. Califano and P. Harrison, *J. Appl. Phys.* **91** (2002) 389.
26. C. H. Edwards Jr. and D. E. Penney, *Calculus and Analytic Geometry*, Chap. 5 (Prentice Hall, Inc., Englewood Cliffs, NJ, 1988), p. 276.
27. J. H. Davies, *J. Appl. Phys.* **84** (1998) 1358.
28. G. S. Pearson and D. A. Faux, *J. Appl. Phys.* **88** (2000) 730.